

Manipulations in Hydrogel Degradation Behavior Enhance Osteoblast Function and Mineralized Tissue Formation

DANIELLE S.W. BENOIT,¹ ANDREW R. DURNEY,¹ and KRISTI S. ANSETH^{1,2*}

ABSTRACT

Hydrogels were prepared by copolymerizing a degradable macromer, poly(lactic acid)-b-poly(ethylene glycol)-b-poly(lactic acid) endcapped with methacrylate groups (PEG-LA-DM), with a non-degradable macromer, poly(ethylene glycol) dimethacrylate (PEGDM). Copolymer networks consisted of 100:0, 83:17, 67:33, and 50:50 PEGDM:PEG-LA-DM mass %, essentially creating scaffolds that exhibit 0, 17, 33, and 50% degradation over the time course of the experiment. Osteoblasts were photoencapsulated in these copolymer hydrogels and cultured for 3 weeks *in vitro*. Metabolic activity, proliferation, and alkaline phosphatase production were enhanced by an increase PEG-LA-DM content and corresponding degradation. Gene expression of the cultured osteoblasts, normalized to β -actin, was analyzed, and osteopontin and collagen type I gene expression increased with degradation. Finally, as a measure of mineralized tissue formation, calcium and phosphate deposition was analyzed biochemically and histologically. Mineralization increased with increasing concentration of PEG-LA-DM and biochemically resembled that of hydroxyapatite.

INTRODUCTION

TOWARD THE END OF DEVELOPING an osteoblast delivery vehicle to enhance bone tissue regeneration, the degradation rate and mass loss profiles of the scaffold are important design parameters. As the scaffold degrades, both the physical and chemical microenvironment experienced by the cells changes. Directly resulting from the degradation, extracellular matrix (ECM) elaborated by the cells fills the void space. Ultimately, if the cellular niche is appropriately engineered, the matrix degrades at the same rate of tissue formation and the final product is native tissue.

Several approaches have been utilized to develop biocompatible and degradable scaffolds for tissue engineering applications. Synthetic polymers such as poly(glycolic acid), poly(lactic acid), and their copolymers PLGA poly(lactide-co-glycolide), originally used as sutures, have gained widespread attention as candidates for tissue

engineering scaffolds.^{1,2} Poly(α -hydroxy esters), such as PLGA, are attractive for applications that rely on hydrolytic degradation at physiological pH, degradation products being resorbed through metabolic pathways, and the potential to tailor the degradation rates. In addition, cells readily attach to films^{3,4} and three-dimensional scaffolds⁵⁻⁷ fabricated from PLGA. Specifically in the field of bone tissue engineering, PLGA scaffolds have been utilized as a delivery vehicle for osteoinductive molecules, including proteins such as basic fibroblast growth factor and genes such as *bmp-2*,⁸⁻¹⁰ and as osteoconductive implants.^{11,12} Although there are many favorable attributes of poly(α -hydroxy esters), limitations still exist with regard to tissue engineering applications due to the necessity of *ex vivo* fabrication. Tissue evolves in pore spaces that are formed during fabrication of woven or macroporous scaffolds. Therefore, scaffold degradation is decoupled from tissue evolution but must occur to result in continuous, native tissue.

¹Department of Chemical and Biological Engineering, University of Colorado, Boulder, Colorado.

²Howard Hughes Medical Institute, University of Colorado, Boulder, Colorado.

Alternatively, many groups are interested in gels that embed cells in a matrix for direct delivery into a tissue defect through *in situ* gelation. Here, there is intimate linkage between degradation of the matrix and distribution of matrix molecules. *In situ* polymerizable macromers eliminate the need for *ex situ* implant fabrication, placement by surgeons is facile and noninvasive, and the filling of irregularly shaped defects is straightforward. Examples of *in situ* forming macromers are based on functionalized poly(propylene fumarate) (PPF), polyanhydride, poly(vinyl alcohol) (PVA), and poly(ethylene glycol) (PEG) systems. *In situ* forming PPF systems have been studied as a bone tissue engineering scaffold.^{13,14} Polyanhydrides, surface-eroding materials, have been utilized in orthopedic^{15,16} and drug delivery applications.¹⁷ PVA hydrogels have been explored as a two-dimensional and three-dimensional cell-culture scaffold.^{18,19} PEG-based systems are a permissive three-dimensional cell culture environment for many cells, including chondrocytes, osteoblasts, mesenchymal stem cells, and islets,^{20–23} and have been designed to incorporate block chemistries that allow for hydrolytic^{20,24} and enzymatic degradation.^{25,26}

Macromolecular monomers composed of PEG with degradable poly(lactic acid) blocks and (meth)acrylate end groups have been explored previously.^{20,21} Histological results related to cartilaginous tissue engineering have shown that gel networks degrading too slowly cause ECM to localize in the pericellular region, although gels that degrade too quickly result in major defects in the developing tissue.^{20,27} Thus, the degradation rate of the gels in which cells are encapsulated has a major effect on cell function and the quantity and quality of tissue evolution. Hydrogel networks formed from multifunctional macromers such as poly(lactic acid)-b-poly(ethylene glycol)-b-poly(lactic acid) endcapped with methacrylate groups (PEG-LA-DM) follow a bulk degradation pathway in which degradation initially advances slowly and somewhat linearly as individual crosslinks are cleaved from the network and diffuse out of the gel. As the crosslinks are broken, the network mesh size increases, and

the diffusion of secreted ECM molecules is enhanced to facilitate macroscopic tissue formation. In addition, the mechanical properties of the gel decrease with degradation. When the weight-average number of crosslinks per kinetic chain (poly-(meth)acrylate) becomes less than two, the network itself can be solubilized, and the remaining mass is lost in one final burst, known as the reverse gel point.²⁸

In this study, hydrogels were prepared by copolymerizing a degradable macromer, PEG-LA-DM, with a slow degrading macromer, poly(ethylene glycol) dimethacrylate (PEGDM). By tailoring the gel composition, gels that erode to various extents of degradation were synthesized, and specifically, copolymer networks consisted of 100:0, 83:17, 67:33, and 50:50 PEGDM:PEG-LA-DM ratios. Osteoblasts were photoencapsulated in the copolymer hydrogels, and osteoblast function, gene expression, and mineralized tissue formation were monitored for 3 weeks to examine the effects of degradation on parameters important in tissue regeneration. These include cell proliferation and activity, expression of ECM proteins, and mineral deposition.

MATERIALS AND METHODS

Macromers

Poly(ethylene glycol) dimethacrylate (PEGDM; MW ~4600) and a tri-block copolymer, poly(lactic acid)-b-poly(ethylene glycol)-b-poly(lactic acid) with methacrylate end groups (PEG-LA-DM; MW ~4600) were synthesized as described elsewhere.²⁹ On average, two lactide repeat units were added to each side of the core PEG molecule (¹H NMR). The chemical structures of these macromers are shown in Fig. 1. Although the PEGDM macromers form hydrogels that are nondegradable on the time scale of these experiments, the lactic acid repeat units of the PEG-LA-DM macromers are hydrolytically degraded.

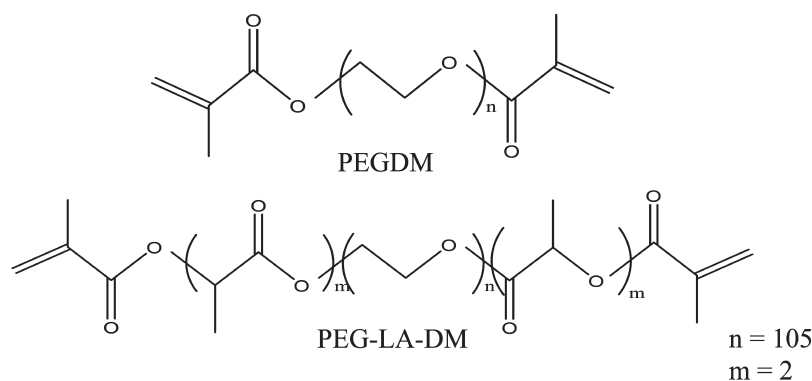


FIG. 1. Chemical structures of the PEG-based macromers.

Hydrogel synthesis and characterization

Hydrogel disks (5 mm in diameter, 2 mm in thickness) consisting of 10wt% PEG-LA-DM with 0.05wt% of 2-hydroxy-1-[4-(hydroxyethoxy) phenyl]-2-methyl-1-propanone (Ciby-Geigy) as a photoinitiator were formed by means of photopolymerization using a long-wave ultraviolet lamp (UVP, model XX-20) at an intensity of ~ 4 mW/cm² for 10 min.³⁰ Hydrogels were degraded in osteoblast complete medium (see below) at 37°C on an orbital shaker and were removed from the medium every 12–24 h to test for the compressive modulus. A previously developed, theoretical model that accounts for structural and kinetic parameters was used to describe the degradation behavior of the PEG hydrogels.²⁸ The compressive modulus (**K**) is proportional to the crosslinking density, which decays exponentially with degradation. Because these are highly swollen gels, the rate of hydrolysis follows pseudo first-order rate kinetics. By combining these relationships, we can obtain the following relationship, $K \propto e^{-6/5k't}$, in which the kinetic time constant, k' , is a model parameter and t is degradation time.²⁸ Using the experimentally determined k' along with structural information related to the gel connectivity, degradation is readily predicted from the model. The model was modified to predict the degradation of copolymerized gels containing degradable ($k' = 0.00004$ min⁻¹) and nondegradable crosslinks ($k' = 0$).

Osteoblast culture and encapsulation

Osteoblasts were isolated from neonatal (<1-day-old) rat calvaria.³ Cells were maintained in osteoblast growth media: Dulbecco's Modified Eagle Medium (Gibco) supplemented with 10% fetal bovine serum (Invitrogen), 1% penicillin/streptomycin (Gibco), 0.25% gentamicin (Gibco), and 0.25% fungizone (Gibco). Osteoblasts after passage 3 were used in this study.

All hydrogels were formulated by dissolving in phosphate-buffered saline (PBS) different ratios of PEGDM and PEG-LA-DM to achieve a final monomer concentration of 10wt%. The co-monomer ratios utilized were 100:0, 83:17, 75:25, and 50:50 of PEGDM:PEG-LA-DM, respectively. Osteoblasts were combined with sterile macromer/initiator solutions at a concentration of 25×10^6 cells/mL and photoencapsulated (same conditions as above). The resulting cell-hydrogel constructs were incubated in 12-well plates. The constructs were cultured for 3 weeks in osteoblast complete media: osteoblast growth media (see above) supplemented with 100 nM dexamethasone, 10 mM β -glycerophosphate, and 0.05 mM ascorbic acid phosphate. Constructs were removed from culture at days 4, 10, and 21 for biochemical and gene expression analysis and at day 21 for histological analysis.

Biochemical analysis of osteoblasts encapsulated in PEGDM:PEG-LA-DM hydrogels

DNA content, which was used as a measure of cell proliferation, was analyzed using the PicoGreen assay (Molecular Probes). At days 4, 10, and 21 constructs were removed from culture; the constructs were rinsed three times with PBS; 0.5 mL of PBS was added; and the samples were manually homogenized and sonicated (Model W-380, Misonix, Inc., Farmingdale, NY) for 1 min. The resulting solution was assayed for DNA content based on the manufacturer's instructions and using a plate reader (Victor², Perkin Elmer).

Metabolic activity of the encapsulated osteoblasts was analyzed at days 4, 10, and 21 with the AlamarBlue assay (Serotec). A 10 vol% solution of AlamarBlue in media was added to the constructs. Active mitochondria convert resazurin, the active ingredient in AlamarBlue, to resorufin, a fluorescent molecule. After 4 h of incubation, the media/AlamarBlue solution was analyzed for fluorescence (excitation at 560 nm, emission at 590 nm) with a plate reader (Victor², Perkin Elmer).

Alkaline phosphatase (ALP) production was measured using an assay based on the change in absorbance of *o*-nitrophenol as it is enzymatically cleaved by ALP. When ALP is present, the substrate solution undergoes a change from colorless to yellow, which can be measured at 405 nm using a spectrophotometer. The sonicated solutions described above were also utilized for this purpose. The assay was performed by combining 100 μ L of sample with 100 μ L of the ALP substrate. At 5-min intervals, the absorbance at 405 nm was measured with a plate reader (Victor², Perkin Elmer); absorbance versus time was a straight line, the slope of which is directly proportional to the concentration of ALP. By performing the assay using known concentrations of ALP in parallel with the samples, the concentrations of ALP for the samples were calculated.

To normalize all the preceding biochemical assays to relative cell number,³¹ an ATP assay (CellTiter-Glo[®] Luminescent Cell Viability Assay, Promega) was utilized per manufacturer's instructions. ATP has a very short half-life and is constant with cell number;³¹ therefore, it is a suitable molecule to normalize cell functions, eliminating trends due to cell number fluctuations. Briefly, CellTiter-Glo[®] reagent was added to the construct in culture medium in parallel with standards. The contents were mixed for 10 min to allow for complete cell lysis, then for an additional 10 min to equilibrate the luminescence signal. Finally, the luminescence was determined in opaque-walled 96-well plates in a plate reader (Victor², Perkin Elmer) and quantified using a standard curve and a plate reader.

TABLE 1. PRIMER AND PROBE SEQUENCES DESIGNED BY BEACON DESIGNER SOFTWARE AND UTILIZED FOR REAL-TIME PCR

Gene	Sense primer	Anti-sense primer	Probe
β -actin	5'-AGCCATGTACGTAGCCATCCA-3'	5'-GTGTGGGTGACCCCGTCTC-3'	5'-CTGTGTTGCCCTGTATGCCTCTGGTCCG-3'
Osteopontin (OPN)	5'-AACTCTTCCAAGCAACTCCAATGA-3'	5'-AATCCTCGCTCTTGCATGGT-3'	5'-TCGTCATCGTCGTCATCATCGTCCA-3'
Collagen type I (COL I)	5'-GGGCAAGACAGTGATTGAATACA-3'	5'-GGATGGAGGGAGTTTACAGGAA-3'	5'-CCAAGTCTCCCCCGCTGCCCATC-3'

Gene expression of osteoblasts encapsulated in PEGDM:PEG-LA-DM hydrogels

Osteoblast gene expression was analyzed using reverse transcription polymerase chain reaction. After days 4, 10, and 21, constructs were removed from culture and rinsed three times with PBS. Total RNA was isolated using a guanidinium thiocyanate/phenol reagent (TRI reagent, Sigma) and standard manufacturer's protocols. After allowing the RNA pellet to dry, it was resuspended in nuclease-free water, and any residual genomic DNA in the samples was digested (DNase I, Invitrogen). RNA was then quantified using the RiboGreen assay (Molecular Probes) based on the manufacturer's instructions and a plate reader (Victor², Perkin Elmer).

Reverse transcription was performed using the iScript cDNA Synthesis Kit (Bio-Rad). A 50-ng total RNA sample was used for the single-strand cDNA synthesis. The reverse transcription reaction was incubated at 25°C for 5 min, 42°C for 30 min, and terminated at 85°C for 5 min. Polymerase chain reaction (PCR) was conducted using the iCycler Real-Time PCR machine (Bio-Rad), and primers and probes were designed using the Beacon Designer primer design program (Table 1). Primers (Invitrogen) and probes (Integrated DNA Technologies) for osteopontin (OPN), collagen type I (COL I), and β -actin were used. The following PCR parameters were utilized: 95°C for 90 s followed by 45 cycles of 95°C for 30 s and 55°C for 60 s. Threshold cycle (C_T) analysis was used to quantify PCR products, normalized to β -actin.

Mineralization by osteoblasts encapsulated in PEGDM:PEG-LA-DM hydrogels

The ability of osteoblasts to secrete a mineralized matrix *in vitro* was assessed histologically. Cell-hydrogel constructs were fixed overnight in 10% formalin (Fisher), transferred to 22wt% sucrose (Aldrich) for 72 h, frozen in Cryo-gel (Instrumedics, Inc.), and cryosectioned (10- μ m sections). The sections were stained using the von Kossa protocol, which stains mineral deposits dark brown or black and with Masson's trichrome, which stains collagen blue. All histological chemicals were obtained from Sigma. Sections were imaged (Nikon Eclipse TE300) and the percent mineralization (percent stained area of von Kossa-stained sections) was quantified using image analysis software (ImageJ).

Further verification of mineralization was performed using calcium and phosphate assays. Constructs were removed from culture at days 4, 10, and 21 and rinsed three times with HEPES buffer solution (Invitrogen). Then, 1 mL 0.9 N H₂SO₄ was added to each well, and plates were incubated overnight at 37°C to dissolve all deposited calcium and phosphate. For the calcium assay, the supernatant, in triplicate, was added to 100 μ L of a solution containing one part calcium binding reagent (0.024wt%

o-cresolphthalein (Sigma) and 0.25wt% 8-hydroxyquinone (Sigma) in diH₂O) and one part calcium buffer (500 mM 2-amino-2-methyl-1,3 propanediol (Aldrich) in diH₂O). The absorbance of each solution was then measured at 560 nm using a plate reader, and based on a standard curve of known concentrations of calcium chloride, the total amount of calcium deposited in each hydrogel was determined. Hydrogels with no encapsulated osteoblasts were also tested, and any subsequent mineral detected was subtracted from the quantity detected in hydrogels with osteoblasts.

To determine the phosphate content of constructs, a previous method was utilized with the same supernatant as above.³² Reagent A consisted of 1.75wt% ammonium heptamolybdate heptahydrate (Aldrich) in 6.3 N H₂SO₄, and Reagent B consisted of 0.035wt% malachite green (Aldrich) and 0.35wt% poly(vinyl alcohol) (Aldrich) in diH₂O. Sample solutions were combined with Reagent A (20 μL) and Reagent B (20 μL) in triplicate in a 96-well plate. After 20 min of incubation at room temperature, the absorbance of each well was measured using a plate reader at 590 nm. Using a range of K₂HPO₄ standards (Sigma), the concentration of phosphate in each gel could be calculated. Combining the calcium assay results with these experiments, the ratios of calcium to phosphate (Ca²⁺:PO₄³⁻) were then determined and compared with native hydroxyapatite.

Statistical analysis

Statistical analysis was performed using a one-way analysis of variance. Data are presented as mean ± standard deviation.

RESULTS

Characterization of degradable hydrogels

PEGDM does not degrade on the time scale of these experiments; however, the PEG-LA-DM degrades completely in 3 weeks *in vitro* after pseudo first-order hydrolysis kinetics of the crosslinks. As the crosslinks are hydrolyzed, the concentration of the crosslinks in the network decays exponentially as a function of time. Fig. 2a shows an ideal schematic of the degrading network structure when a portion of the crosslinks is degradable. In addition, the percent degradation from hydrogels was predicted using a previously developed theoretical model in which the hydrolysis kinetics (a model parameter) were based on experimental compressive moduli (K) that were measured as a function of degradation time for gels prepared from 10wt% PEG-LA-DA, as in Bryant *et al.*,^{27,33} shown in Fig. 2b. The model was modified to predict from the experimentally obtained modulus data the degradation behavior of copolymerized gels containing

degradable and nondegradable crosslinks. The predicted mass-loss behavior as a function of degradation and composition of the hydrogels (Fig. 2c) shows that when a higher percentage of crosslinks is nondegradable, the rate of degradation decreases at any give time point.

Biochemical analysis of osteoblasts encapsulated in PEGDM:PEG-LA-DM hydrogels

To monitor biochemical activity of osteoblasts encapsulated in various PEGDM:PEG-LA-DM copolymer gels, proliferation, metabolic activity, and ALP production assays were employed. Proliferation, as determined by the total amount of DNA normalized by a relative measure of cell number (ATP/gel), was measured, and results are shown in Fig. 3a. Generally, proliferation increased with increasing degradation. When comparing data at day 4 versus day 10, there is an increase in proliferation and also at each of the days, proliferation increased with respect to an increase in PEG-LA-DM concentration. Interestingly, at day 21, when the degradation is nearly complete, there is a decrease in proliferation indicating that proliferation is coupled to degradation in a complex temporal manner.

Metabolic activity, utilizing the AlamarBlue assay, was determined at days 4, 10, and 21, and the results shown in Fig. 3b were normalized to a relative measure of cell number (ATP/gel). Metabolic activity, a general cell function measure, was relatively constant at the early stages of degradation (4 and 10 days) for all compositions but increased dramatically at later stages (21 days) with the highest concentrations of PEG-LA-DM (*i.e.*, the greatest degradation).

As a final and more specific measure of osteoblast activity, ALP production was monitored at days 4, 10, and 21, and the results shown in Fig. 3c were normalized to a relative measure of cell number (ATP/gel). ALP production was highly coupled to degradation. For a given time, ALP production increased with increased PEG-LA-DM concentration. In addition, at a composition of 67:33 PEGDM:PEG-LA-DM, there is more than a twofold increase of ALP production from 4 to 21 days.

Gene expression of osteoblasts encapsulated in PEGDM:PEG-LA-DM hydrogels

Gene expression profiles for the cultured osteoblasts, normalized to β-actin, were quantified over time with gel composition and illustrated in Fig. 4. OPN (Fig. 4a), and collagen type I, COL I (Fig. 4b), gene expression followed similar trends where an increase occurred in response to an increase concentration of PEG-LA-DM and degradation. Cells encapsulated in the 50:50 composition exhibited an average of 10× and 4× greater expression for OPN and COL I, respectively, when compared to the 100:0 composition at all time points.

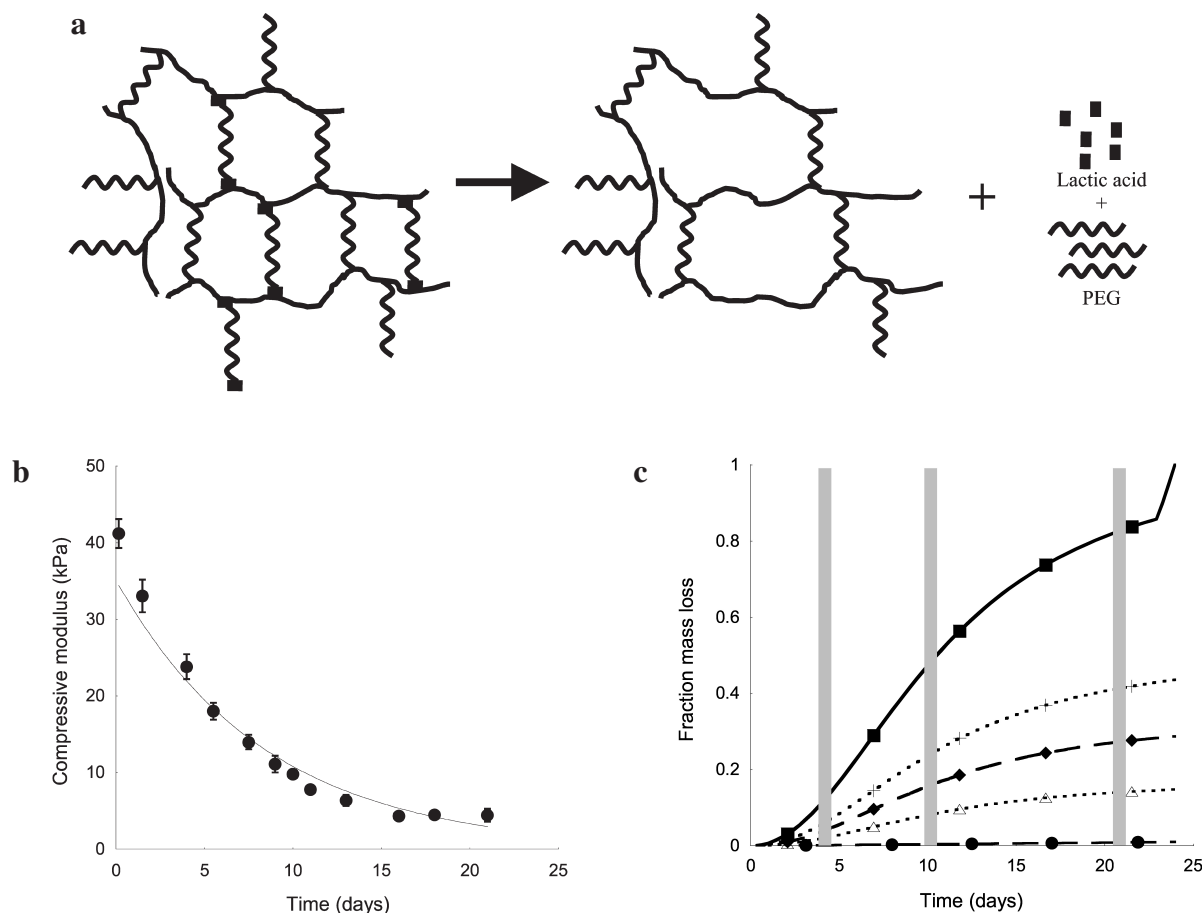


FIG. 2. An ideal schematic (a) of the degradation of hydrogels formed by copolymerizing macromers that do not degrade on the time scale of the experiment (PEGDM) with macromers that degrade completely in 3 weeks (PEG-LA-DM). Compressive modulus (b) experimentally determined for 100% PEG-LA-DM gels and fraction mass loss (c) as a function of degradation time and gel composition as predicted from a theoretical model^{27,28} based on k' from compressive modulus data for gels prepared from 100% PEGDM (dashed line with closed circles), 100% PEG-LA-DM (solid line with solid squares), and from varying ratios of PEGDM:PEG-LA-DM (83:17 (dashed line with crosses), 67:33 (dashed line with closed diamonds), and 50:50 (dashed line with open triangles)). Gray areas indicate when functions of encapsulated osteoblasts were measured.

Interestingly, OPN expression was relatively constant with time, but strongly dependent on the gel composition. Conversely, COL I expression was greatest at day 10 for the two highest PEG-LA-DM-containing hydrogels, indicating a temporal expression pattern of the two gene products.

Mineralization by osteoblasts encapsulated in PEGDM:PEG-LA-DM hydrogels

Von Kossa and Masson's Trichrome-stained histological sections of photoencapsulated osteoblasts in PEG hydrogels after 21 days of *in vitro* culture are shown in Fig. 5a, and mineralization is quantified in Fig. 5b. These procedures stain mineral deposits brown to black and collagen blue. As expected, collagen and mineral deposits are localized in the pericellular envi-

ronment for the slow-degrading gels. However, with increasing concentration of PEG-LA-DM allowing for increased degradation, the diffusion of collagen is increased and subsequent mineralization is more uniform throughout the gel when compared to the 100:0 composition. In addition, as the concentration of PEG-LA-DM increases, the overall percentage of mineralization is increased. For instance, mineralization is almost 3× greater for cells encapsulated in the 50:50 versus the 100:0 composition.

Although mineralization can be enhanced by increasing concentration of PEG-LA-DM in hydrogels, the composition of the mineral phase is important to characterize. Using an assay specific for calcium and phosphate, the absolute amounts of these minerals and the $\text{Ca}^{2+}:\text{PO}_4^{3-}$ ratios were determined for the hydrogels at days 4, 10, and 21, and the results are shown in

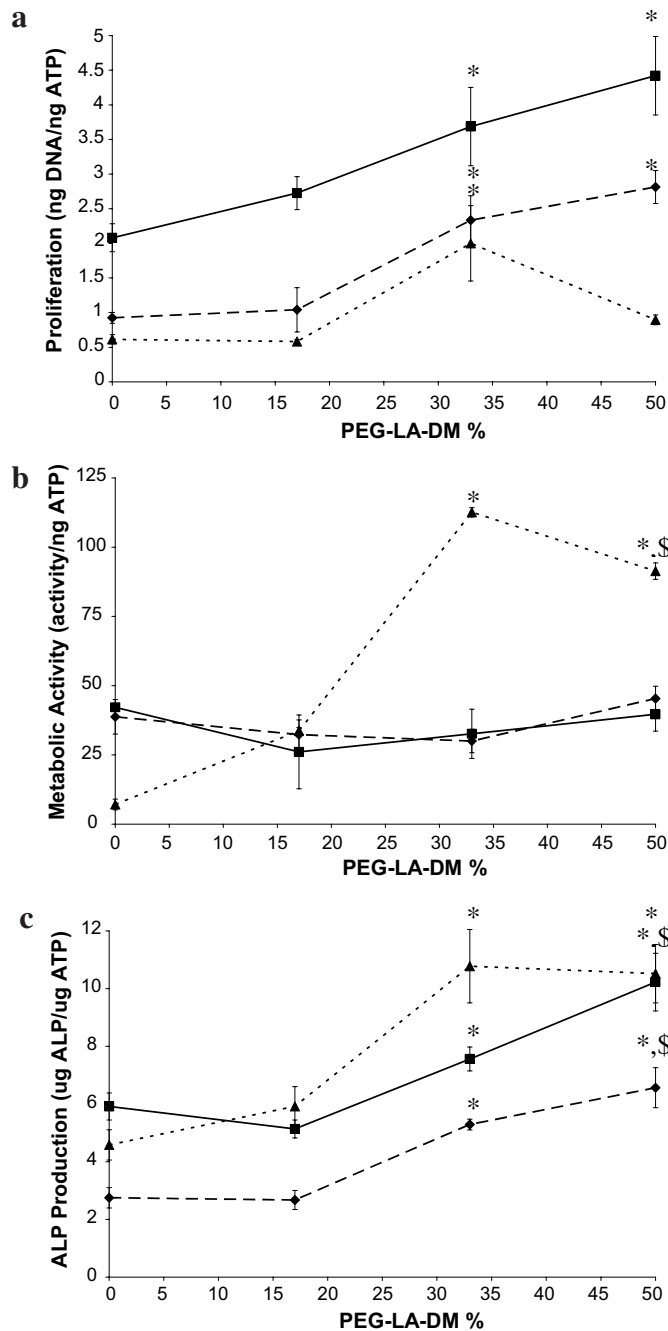


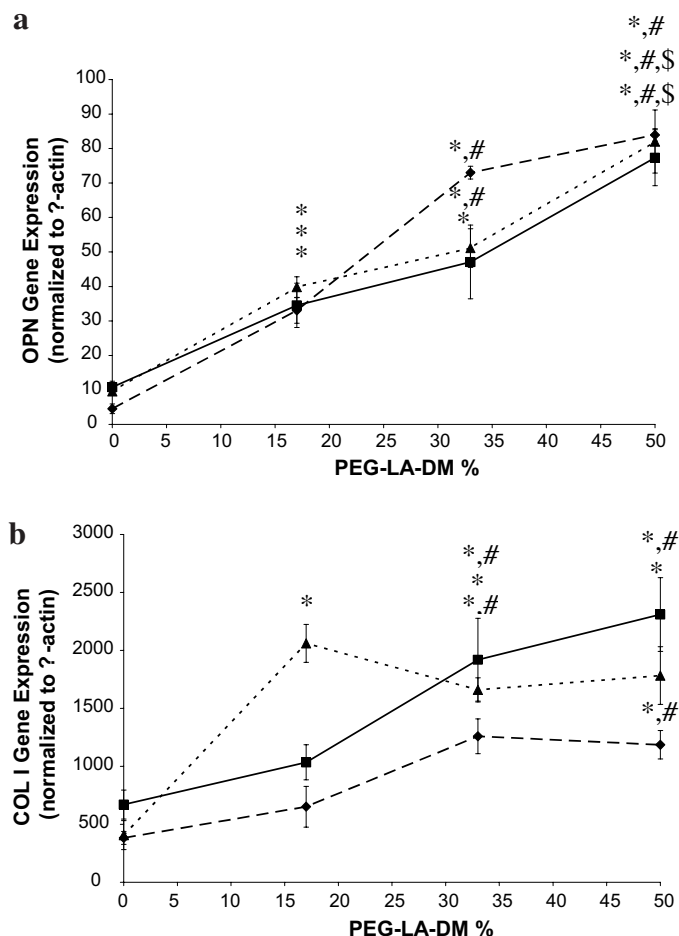
FIG. 3. Proliferation (a), metabolic activity (b), and alkaline phosphatase (ALP) production (c) of osteoblasts encapsulated in increasing concentrations of PEG-LA-DM in copolymers of PEGDM:PEG-LA-DM after 4 days (dashed line with diamonds), 10 days (solid line with squares), and 21 days (dashed line with triangles (error bars designate standard deviation). **p* < 0.05 of sample versus control (10% PEGDM) at that timepoint, \$*p* < 0.05 of sample versus 67:33 composition at that timepoint. *n* = 3 samples per condition.

Fig. 6. Calcium and phosphate deposition increased with increasing concentration of PEG-LA-DM at all time points. The greatest difference in calcium and phosphate deposition is found on day 4. By day 10, all PEG-LA-DM inclusive constructs have statistically the same concentration of mineral phase. Calcium and phosphate deposition increases with increasing culture time, however, with a slower rate as the study progresses. In addition, the $Ca^{2+}:PO_4^{3-}$ ratios were roughly 1.6, the ratio expected for crystalline hydroxyapatite ($Ca_{10}(PO_4)_6(OH)_2$).^{34,35}

DISCUSSION

In the field of bone tissue regeneration, the physical and biochemical consequences of gel degradation profiles on encapsulated osteoblasts are critically important. By fabricating hydrogels through the copolymerization of macromers with varying mass erosion profiles, networks can be formed that span a wide range of properties during degradation. In this study, osteoblasts were photoencapsulated in hydrogels formed by copolymerizing PEGDM with PEG-LA-DM in varying ratios (100:0, 83:17, 67:33,

FIG. 4. Osteopontin (OPN) (a) and collagen type I (COL I) (b) gene expression normalized to levels of β -actin of osteoblasts encapsulated in increasing concentrations of PEG-LA-DM in copolymers of PEGDM:PEG-LA-DM after 4 days (dashed line with diamonds), 10 days (solid line with squares), and 21 days (dashed line with triangles) (error bars designate standard deviation). * $p < 0.05$ of sample versus control (10% PEGDM) at that timepoint, # $p < 0.05$ of sample versus 83:17 composition at that timepoint, \$ $p < 0.05$ of sample versus 67:33 composition at that timepoint. $n = 3$ samples per condition.



and 50:50 PEGDM:PEG-LA-DM). PEGDM does not degrade on the time scale of these experiments,³⁶ but the ester linkage will cleave over time *in vivo*. PEG-LA-DM used in this study degrades completely in ~ 3 weeks *in vitro* following pseudo-first-order hydrolysis kinetics of the crosslinks.²⁸ By comparing cell function biochemically, gene expression, and mineralized tissue formation in these gels, we aim to understand the influence of gel degradation on the secretory properties of cells and ECM deposition, and ultimately, tissue evolution. Interestingly, increasing concentrations of PEG-LA-DM stimulated osteoblasts biochemically, increasing metabolic activity, proliferation, and ALP production. In addition, gene expression of OPN and COL I were augmented. Finally, when exploring mineralization histologically and biochemically, the networks with higher concentration of PEG-LA-DM, thus degradation, exhibited the greatest mineralization.

Degradation of the PEG gels can be controlled by incorporating slowly degrading crosslinks into the network. When a portion of the crosslinks is slow-degrading and, on average, more than two crosslinks are connected to each kinetic chain, the network will not dissolve. When a higher percentage of crosslinks do not degrade over the time course of the experiment, the rate of degradation decreases. In copolymer gels, the concentration of crosslinks

in the network decays exponentially as a function of time, releasing lactic acid byproducts, among others, until only the PEG crosslinks remain.

In vitro cultures of osteoblasts encapsulated in PEGDM:PEG-LA-DM hydrogels follow the general osteogenic differentiation process with enhancement of various differentiation markers. In general, differentiation begins with an increase in cell density, continues with augmented protein levels including ALP, and culminates with mineralization of a matrix secreted by osteoblasts.³⁷ *In vitro* PEGDM:PEG-LA-DM encapsulated cultures of osteoblasts follow this differentiation process with enhancement of proliferation through day 10, when the cells become quiescent. In addition, ALP production is stimulated and gene expression follows the generalized temporal trend, starting with an increase in OPN, followed by a heightened production of COL I, which continues at a high level until mineralization proceeds.³⁷ Interestingly, the traditional biphasic ALP production seen as osteoblasts mature does not occur in this system, likely due to the conclusion of the study prior to the second increase in ALP production.

Mineralization is increased in response to the increased concentration of PEG-LA-DM in the cell-hydrogel constructs. The mineralized tissue that was formed resem-

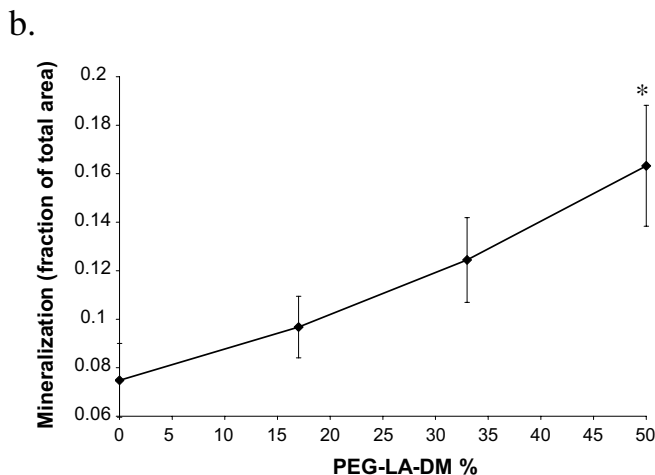
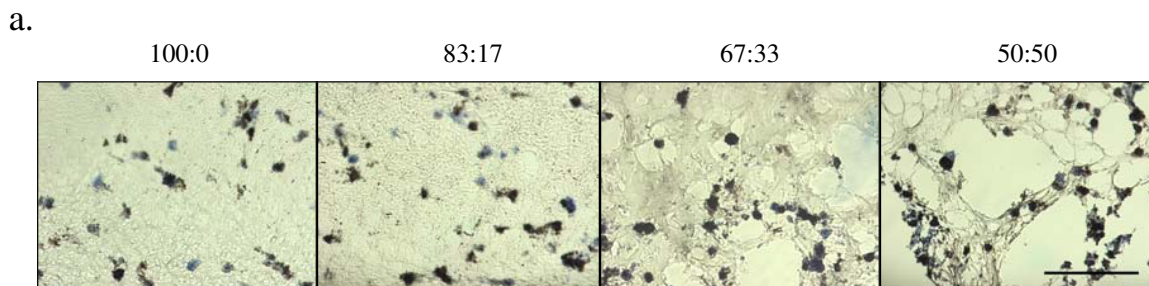


FIG. 5. Light micrographs (a) of von Kossa (mineralization–brown to black) and Masson’s trichrome (collagen–blue) staining (bar = 100 μm) and quantification of mineralization (b) of histological sections of osteoblasts encapsulated in increasing concentrations of PEG-LA-DM in copolymers of PEGDM:PEG-LA-DM after 21 days. **p* < 0.05 of sample versus control (10% PEGDM) at that timepoint. *n* = 3 samples per condition.

bled hydroxyapatite, the mineral phase of bone. In this system, the $\text{Ca}^{2+}:\text{PO}_4^{3-}$ ratio was found to be around 1.6, the ratio found in bone^{34,35} for all copolymer ratios and all times. The $\text{Ca}^{2+}:\text{PO}_4^{3-}$ ratios in amorphous calcium phosphate ($\text{Ca}_3(\text{PO}_4)_2$), brushite ($(\text{CaHPO}_4)_3\text{-H}_2\text{O}$), and octacalcium phosphate ($\text{Ca}_8(\text{PO}_4)_6\text{H}_2$) are 1:0.67, 1:1, and 1:0.75, respectively. These results indicate that the mineralized regions of PEG hydrogels have composition similar to native bone apatite.

It is well known that cells respond to many categories of physiochemical cues, including topographical, chemical, and mechanical ones. In the system described here,

as the hydrogel degrades and crosslinks are hydrolyzed (see Fig. 2), network properties, such as gel mechanics, change. The impact of material mechanics on cell behavior is widely investigated and has significant importance. For instance, Wang *et al.* found that substrate stiffness could be used to modulate cell behavior. Reduced spreading and greater motility of fibroblasts was found on soft polyacrylamide (PAAM) substrates compared to relatively stiffer PAAM.³⁸ In addition, the mechanical properties (for example, rigidity) of the substrate to which a cell adheres have been found to mediate many aspects of cell function including proliferation, migration, and

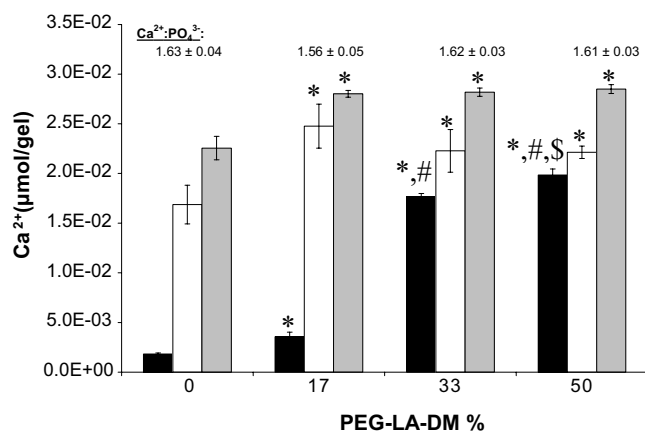


FIG. 6. Calcium deposition and $\text{Ca}^{2+}:\text{PO}_4^{3-}$ ratios by osteoblasts encapsulated in increasing concentrations of PEG-LA-DM in copolymers of PEGDM:PEG-LA-DM after 4 days (black), 10 days (white), and 21 days (gray) (error bars designate standard deviation). **p* < 0.05 of sample versus control (10% PEGDM) at that timepoint; #*p* < 0.05 of sample versus 83:17 composition at that timepoint; \$*p* < 0.05 of sample versus 67:33 composition at that timepoint. *n* = 3 samples per condition.

differentiation, and this suggests that the mechanics of the adhesion substrate may regulate a cell's ability to uptake exogenous signaling molecules.³⁹⁻⁴² A critical role for the rigidity of the cell adhesion substrate on the level of gene transfer and expression has also been found.⁴³

In normal fracture healing, the microenvironment is known to be acidic, likely in combination with elevated lactic acid levels. These conditions result in increased osteoblast activity.⁴⁴ Interestingly, in the results described here, osteoblast biochemical function, gene expression, and mineralization were upregulated in response to increased mass loss, which corresponds to compositions that resulted in greater degradation and release of lactic acid. The maximum possible concentrations of lactic acid in the gels range from 0 to 0.04 M; however, the lactic acid is released over about 3 weeks, resulting in much lower dosing than in a burst release situation. In this study, the degradation and acid byproduct effects are coupled. In work done by Cusack and others,⁴⁵ osteoblast ALP production was increased with increasing concentration of acidic molecules. In addition, in seeding experiments utilizing homopolymer networks of PEG-LA-DM hydrogels, osteoblast ALP production is augmented with a greater number of lactic acid repeats, and thus greater potential for lactic acid release.²⁴ Furthermore, when ascorbic acid is utilized as lactic acid is here, as part of the crosslinker, and osteoblasts are cultured on the scaffolds, both cell proliferation and ALP production are enhanced.⁴⁶

Thus, both biophysical and biochemical factors couple to influence osteoblast function in PEG-LA-DM gels. Degradation leads to increasing porosity facilitating the diffusion and deposition of cell-secreted molecules. However, degradation releases lactic acid byproducts, which can partially influence cell secretory properties and other functions. By careful design of hydrogel cell carriers with rationally targeted modifications and degradation behavior, niches can be synthesized that actively promote cell function, gene expression, and mineralization.

ACKNOWLEDGMENTS

This work has been supported by a grant from the National Institutes of Health (DE016523). Fellowship assistance to D.S.W.B. is awarded graciously from the U.S. Department of Education's Graduate Assistantships in Areas of National Need program, the American Association of University Women, and the National Science Foundation.

REFERENCES

- Behraves, E., Yasko, A.W., Engel, P.S., and Mikos, A.G. Synthetic biodegradable polymers for orthopaedic applications. *Clin. Orthop.* **367**, S118, 1999.
- Freed, L.E., Martin, I., and Vunjak-Novakovic, G. Frontiers in tissue engineering—in vitro modulation of chondrogenesis. *Clin. Orthop.* **367**, S46, 1999.
- Ishaug, S.L., Yaszemski, M.J., Bizios, R., and Mikos, A.G. Osteoblast function on synthetic biodegradable polymers. *J. Biomed. Mater. Res.* **28**, 1445, 1994.
- Ishaug, S.L., Payne, R.G., Yaszemski, M.J., Aufdemorte, T.B., Bizios, R., and Mikos, A.G. Osteoblast migration on poly(alpha-hydroxy esters). *Biotech. Bioeng.* **50**, 443, 1996.
- Shea, L.D., Wang, D., Franceschi, R.T., and Mooney, D.J. Engineered bone development from a pre-osteoblast cell line on three-dimensional scaffolds. *Tissue Eng.* **6**, 605, 2000.
- Ishaug-Riley, S.L., Crane-Kruger, G.M., Yaszemski, M.J., and Mikos, A.G. Three-dimensional culture of rat calvarial osteoblasts in porous biodegradable polymers. *Biomaterials* **19**, 1405, 1998.
- Holy, C.E., Shoichet, M.S., and Davies, J.E. Engineering three-dimensional bone tissue in vitro using biodegradable scaffolds: Investigating initial cell-seeding density and culture period. *J. Biomed. Mater. Res.* **51**, 376, 2000.
- Riddle, K.W., Anseth, K.S., and Mooney, D.J. Controlling DNA expression by modifying the proliferative state of target cells. In preparation, 2006.
- Kirker-Head, C.A., Gerhart, T.N., Armstrong, R., Schelling, S.H., and Carmel, L.A. Healing bone using recombinant human bone morphogenetic protein 2 and copolymer. *Clin. Orthop.* **349**, 205, 1998.
- Mori, M., Isobe, M., Yamazaki, Y., Ishihara, K. and Nakabayashi, N. Restoration of segmental bone defects in rabbit radius by biodegradable capsules containing recombinant human bone morphogenetic protein-2. *J. Biomed. Mater. Res.* **50**, 191, 2000.
- Goldstein, A.S., Zhu, G.M., Morris, G.E., Meszlenyi, R.K., and Mikos, A.G. Effect of osteoblastic culture conditions on the structure of poly(dl-lactic-co-glycolic acid) foam scaffolds. *Tissue Eng.* **5**, 421, 1999.
- Zhang, R.Y., and Ma, P.X. Poly(alpha-hydroxyl acids) hydroxyapatite porous composites for bone-tissue engineering. I. Preparation and morphology. *J. Biomed. Mater. Res.* **44**, 446, 1999.
- Peter, S.J., Miller, S.T., Zhu, G.M., Yasko, A.W., and Mikos, A.G. In vivo degradation of a poly(propylene fumarate) beta-tricalcium phosphate injectable composite scaffold. *J. Biomed. Mater. Res.* **41**, 1, 1998.
- Temenoff, J.S., and Mikos, A.G. Injectable biodegradable materials for orthopedic tissue engineering. *Biomaterials* **21**, 2405, 2000.
- Burkoth, A.K., Burdick, J., and Anseth, K.S. Surface and bulk modifications to photocrosslinked polyanhydrides to control degradation behavior. *J. Biomed. Mater. Res.* **51**, 352, 2000.
- Muggli, D.S., Burkoth, A.K., Keyser, S.A., Lee, H.R., and Anseth, K.S. Reaction behavior of biodegradable, photocross-linkable polyanhydrides. *Macromolecules* **31**, 4120, 1998.
- Leong, K.W., Brott, B.C., and Langer, R. Bioerodible polyanhydrides as drug-carrier matrices. I. Characterization, degradation, and release characteristics. *J. Biomed. Mater. Res.* **19**, 941, 1985.

18. Nuttelman, C.R., Mortisen, D.J., Henry, S.M., and Anseth, K.S. Attachment of fibronectin to poly(vinyl alcohol) hydrogels promotes nih3t3 cell adhesion, proliferation, and migration. *J. Biomed. Mater. Res.* **57**, 217, 2001.
19. Schmedlen, K.H., Masters, K.S., and West, J.L. Photocrosslinkable polyvinyl alcohol hydrogels that can be modified with cell adhesion peptides for use in tissue engineering. *Biomaterials* **23**, 4325, 2002.
20. Bryant, S.J., and Anseth, K.S. Hydrogel properties influence ECM production by chondrocytes photoencapsulated in poly(ethylene glycol) hydrogels. *J. Biomed. Mater. Res.* **59**, 63, 2002.
21. Burdick, J.A., and Anseth, K.S. Photoencapsulation of osteoblasts in injectable RGD-modified PEG hydrogels for bone tissue engineering. *Biomaterials* **23**, 4315, 2002.
22. Nuttelman, C.R., Tripodi, M.C., Anseth, K.S. Synthetic hydrogel niches that promote hMSC viability. *Matrix Biol.* **24**, 208, 2005.
23. Williams, C.G., Malik, A.N., Kim, T.K., Manson, P.N., and Elisseff, J.H. Variable cytocompatibility of six cell lines with photoinitiators used for polymerizing hydrogels and cell encapsulation. *Biomaterials* **26**, 1211, 2005.
24. Burdick, J.A., Mason, M.N., and Anseth, K.S. In situ forming lactic acid based orthopaedic biomaterials: Influence of oligomer chemistry on osteoblast attachment and function. *J. Biomat. Sci. Polym. Ed.* **12**, 1253, 2001.
25. Gobin, A.S., and West, J.L. Cell migration through defined, synthetic extracellular matrix analogues. *FASEB J.* **751**, 16, 2002.
26. Lutolf, M.R., Weber, F.E., Schmoekel, H.G., Schense, J.C., Kohler, T., Muller, R., and Hubbell, J.A. Repair of bone defects using synthetic mimetics of collagenous extracellular matrices. *Nature Biotechnol.* **21**, 513, 2003.
27. Bryant, S.J., and Anseth, K.S. Controlling the spatial distribution of ECM components in degradable peg hydrogels for tissue engineering cartilage. *J. Biomed. Mater. Res. A* **64A**, 70, 2003.
28. Metters, A.T., Anseth, K.S., and Bowman, C.N. Fundamental studies of a novel, biodegradable PEG-b-PLA hydrogel. *Polymer* **41**, 3993, 2000.
29. Sawhney, A.S., Pathak, C.P., and Hubbell, J.A. Bioerodible hydrogels based on photopolymerized poly(ethylene glycol)-co-poly(alpha-hydroxy acid) diacrylate macromers. *Macromolecules* **26**, 581, 1993.
30. Bryant, S.J., Nuttelman, C.R., and K.S. Anseth. Cytocompatibility of UV and visible light initiating systems on cultured NIH/3T3 fibroblasts in vivo. *J. Biomat. Mater. Sci. Polymer Ed.* **11**, 439, 2000.
31. Petty, R.D., Sutherland, L.A., Hunter, E.M., and Cree, I.A. Comparison of MTT and ATP-based assays for the measurement of viable cell number. *J. Biolum. Chemilum.* **10**, 29, 1995.
32. Van Veldhoven, P.P., and Mannaerts, G.P. Inorganic and organic phosphate measurements in the nanomolar range. *Anal. Biochem.* **161**, 45, 1987.
33. Martens, P., Metters, A.T., Anseth, K.S., and Bowman, C.N. A generalized bulk-degradation model for hydrogel networks formed from multivinyl cross-linking molecules. *J. Phys. Chem. B* **105**, 5131, 2001.
34. Murphy, W.L., and Mooney, D.J. Bioinspired growth of crystalline carbonate apatite on biodegradable polymer substrata. *J. Am. Chem. Soc.* **124**, 1910, 2002.
35. Song, J., Saiz, E., and Bertozzi, C.R. A new approach to mineralization of biocompatible hydrogel scaffolds: An efficient process toward 3-dimensional bonelike composites. *J. Am. Chem. Soc.* **125**, 1236, 2003.
36. Larsen, I.B., and Munksgaard, E.C. Effect of human saliva on surface degradation of composite resins. *Scand. J. Dent. Res.* **99**, 254, 1991.
37. Stein, G.S., Lian, J.B., and Owen, T.A. Relationship of cell-growth to the regulation of tissue-specific gene-expression during osteoblast differentiation. *FASEB J.* **4**, 3111, 1990.
38. Pelham, R.J., and Wang, Y.L. Cell locomotion and focal adhesions are regulated by substrate flexibility. *Proc. Natl. Acad. Sci. USA* **94**, 13661, 1997.
39. Galbraith, C., and Sheetz, M.P. Forces on adhesive contacts affect cell function. *Curr. Opin. Cell Biol.* **10**, 566, 1998.
40. Wang, H.B., Dembo, M., and Wang, Y.L. Substrate inflexibility regulates growth and apoptosis of normal but not transformed cells. *Am. J. Physiol. Cells* **279**, C1345, 2000.
41. Engler, A.J., Griffin, M.A., Sen, S., Bonnetmann, C.G., Sweeney, H.L., and Discher, D.E. Myotubes differentiate optimally on substrates with tissue-like stiffness: pathological implications for soft or stiff microenvironments. *J. Cell Biol.* **166**, 877, 2004.
42. Kohn, H.J., Polte, T., Alsborg, E., and Mooney, D.J. FRET measurements of cell-tractions forces and nano-scale clustering of adhesion ligands varied by substrate stiffness. *Proc. Natl. Acad. Sci. USA* **102**, 4300, 2005.
43. Kong, H.J., Liu, J., Riddle, K., Matsumoto, T., Leach, K., and Mooney, D.J. Non-viral gene delivery regulated by stiffness of cell adhesion substrates. *Nature Mater.* **4**, 460, 2005.
44. Spector, J.A., Mehrara, B.J., Greenwald, J.A., Saadeh, P.B., Steinbrech, D.S., Bouletreau, P.J., Smith, L.P., and Longaker, M.T. Osteoblast expression of vascular endothelial growth factor is modulated by the extracellular microenvironment. *Am. J. Physiol. Cell Physiol.* **280**, C72, 2001.
45. Cusack, S., Jewell, C., and Cashman, K.D. The effect of conjugated linoleic acid on the viability and metabolism of human osteoblast-like cells. *Prost. Leuk. Ess. Fatty Acids* **72**, 29, 2005.
46. Zhang, J.Y., Doll, B.A., Beckman, E.J., and Hollinger, J.O. A biodegradable polyurethane-ascorbic acid scaffold for bone tissue engineering. *J. Biomed. Mater. Res. A* **67A**, 389, 2003.

Address reprint requests to:

*Kristi Anseth
Department of Chemical and Biological Engineering
University of Colorado
Boulder, CO 80309-0424*

E-mail: kristi.anseth@colorado.edu

